Journal of the European Ceramic Society **15** (1995) 513–520

0955-2219/95/$9.50

0955-2219(95)00017-8

Creep Properties of Single Crystal Oxides Evaluated by a Larson–Miller Procedure

Shiqiang Deng* & Richard Warren

Department of Materials Science and Production Technology, Luleå University, S-971 87 Luleå, Sweden

(Received 1 June 1994; revised version received 22 September 1994; accepted 26 January 1995)

Abstract

A collation of published results of compressive and tensile creep studies of single and binary oxide single crystals is presented. For the purposes of comparison the results were normalised by means of a Larson–Miller procedure. This method proved to be effective in providing a ranking of the oxides in terms of their creep resistance. Binary oxides with complex crystal structures exhibited the highest creep strengths; no direct correlation with the melting point could be found.

1 Introduction

Composites consisting of an oxide matrix reinforced with continuous oxide fibres are beginning to attract attention in the search for materials capable of withstanding higher temperatures than currently available materials. Thus, many oxides can provide the oxidation-resistance, high melting point and low density that are essential for high temperature aerospace applications. On the other hand, polycrystalline ceramic oxides do not exhibit adequate creep-resistance and high temperature strength. However, several studies have shown that certain single crystal oxides may be capable of providing good creep-resistance and strength; presumably because they lack grain boundaries which are a source of weakness at high temperatures.

Many isolated studies have been made of the creep behaviour of various single crystal oxides, but as far as the present authors are aware, no attempt has been made to carry out an exhaustive, systematic compilation of these. The purpose of the present work was to gather creep data from the many sources for both single and binary oxides in order to assess their relative creep resistance. A direct comparison of creep results from different sources is usually not straightforward since they have usually been obtained under different test conditions, for example, with different combinations of temperature and stress. Moreover, for oxides exhibiting large differences in creep resistance, the position of the stress–temperature regimes employed can vary significantly. To make a meaningful comparison of creep resistance in these cases, the creep data was evaluated here on the basis of a Larson–Miller normalisation procedure[1] as will be outlined in the next section.

Studies of the creep of single crystal oxides have been reported for both compressive and tensile loading and these are treated separately in this paper.

2 Larson–Miller Procedure for Creep Data Evaluation

The basis of the Larson–Miller treatment is that the creep process can be considered to be thermally activated and consequently for a given applied stress the creep rate is described by an Arrhenius-type expression of the form:

$$\dot{\epsilon}_s = A\exp(-Q/RT) \tag{1}$$

where $\dot{\epsilon}_s$ is the steady state creep rate, Q is the activation energy for the creep process, T is the absolute temperature in Kelvin, R is the gas constant and A is a constant. Equation (1) can also be written as

$$Q/R = T(\ln A - \ln \dot{\epsilon}_s) \tag{2}$$

Introducing the concept of a creep life, t_S, defined as the time taken for the steady state creep rate to yield a given arbitrary strain, ϵ_x:

$$t_s = \epsilon_x/\dot{\epsilon}_s \tag{3}$$

Equation (2) can then be written:

$$L = Q/R = T(C + \log t_s) \tag{4}$$

*Permanent address: Third Department, Central Iron and Steel Research Institute, 100081 Beijing, China.

where L is the so-called Larson–Miller parameter and C is a constant. Assuming Q to be independent of temperature, the value of L at a given stress for a given material is considered to be constant, which implies that there is a fixed relationship between T and t_S. Moreover it is generally found that L is inversely proportional to log σ, the applied stress. Thus, L values derived from creep experiments carried out at different combinations of stress and temperature can be plotted against log σ to yield a single straight line. Creep data appropriate to other combinations of stress–temperature–lifetime can then be predicted from the Larson–Miller plot by interpolation or extrapolation. For example, in the present work, the Larson–Miller plots were used to derive a 'creep strength' defined as the stress required at 1600°C to produce a strain, ϵ_x, of 10^{-5} in a time, t_S, of 10^4 s, (i.e. $\dot{\epsilon}_s = 10^{-9}$).

The derived relationship between σ, t_S and T is relatively insensitive to the value of the constant C and it is often set at a fixed value when considering a group of related materials. However, in this work, whenever sufficient experimental data was available, an individual value of C was determined for each oxide, being extracted from a plot of log t_S versus $1/T$ on the basis of a rearrangement of eqn (4):

$$\log t_s = -C + \text{constant}/T \qquad (5)$$

In the present Larson–Miller treatment of published data, values of strain rate corresponding to a steady state were sought, care being taken to avoid values corresponding to primary stages of creep. The values were taken either as reported explicitly or estimated from the published creep curves.

3 Results

Representative plots of log t_S versus $1/T$ used to derive C values are shown in Figs 1 and 2 for ThO_2 and Al_2O_3 single crystals. Several Larson–Miller plots for different oxides are presented in Figs 3–7. Derived C values and values of creep strength together with test details and source references are collected in Tables 1 and 2 for compressive and tensile loading respectively.

It was found that the log t_S versus $1/T$ plots for a given oxide and crystal orientation at different stresses yielded C values with relatively small variations as can be seen from Figs 1 and 2; in these cases average values were used. In some instances small differences in slope were observed (Fig. 2) indicating a variation in the activation energy, Q. This effect was neglected and again an average value of C was used.

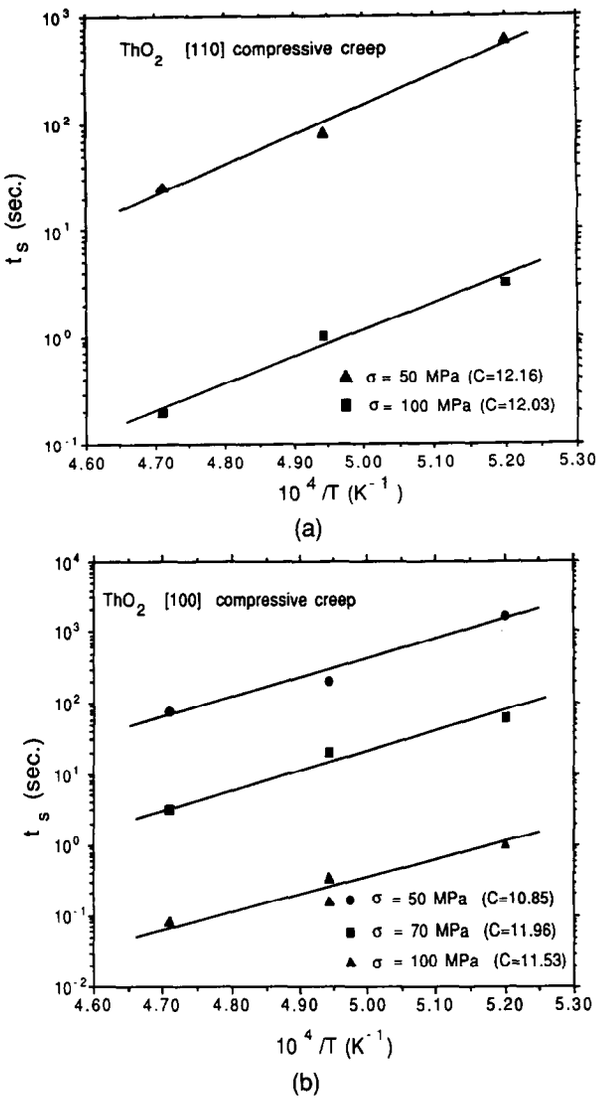

Fig. 1. Plot of log(t_s) versus ($1/T$) of ThO_2 single crystal: (a) [110]; (b) [100].

Figures 3–7 show L values derived from the stated C values using eqn (4) plotted versus the corresponding values of logarithm of applied stress. Linear regression was used to construct the

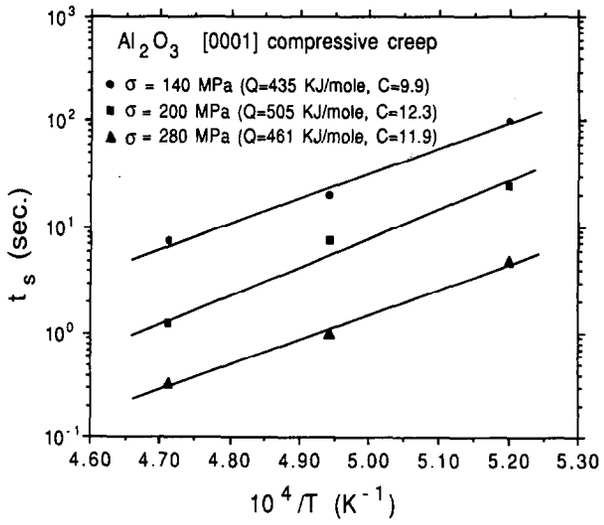

Fig. 2. Log(t_s) versus ($1/T$) of sapphire single crystal for compressive creep.

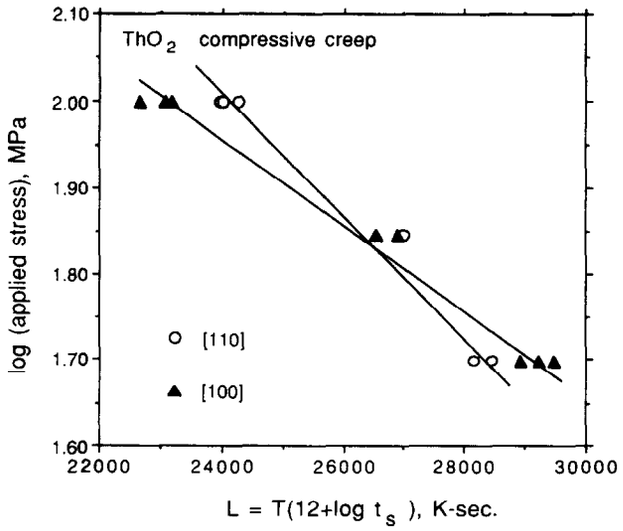

Fig. 3. Larson–Miller plot of ThO_2 single crystal (compressive creep).

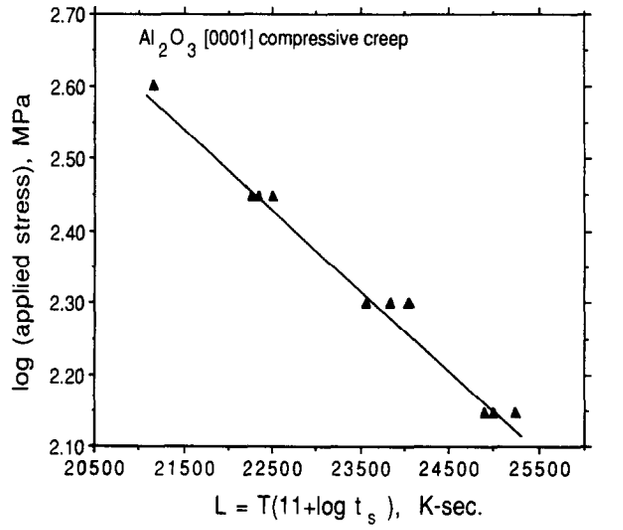

Fig. 4. Larson–Miller plot of single crystal sapphire (compressive creep).

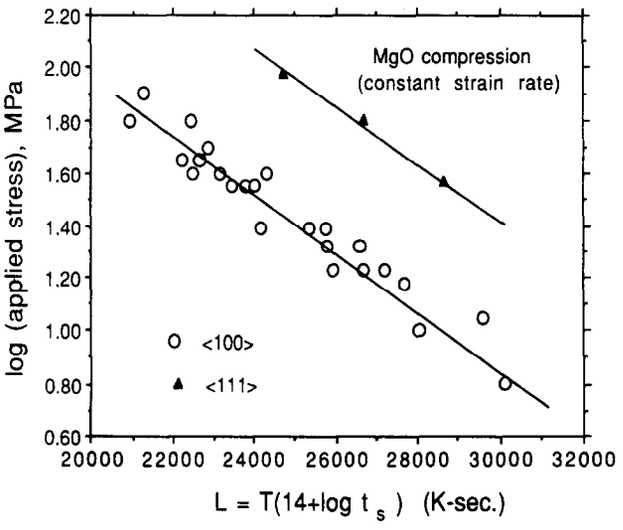

Fig. 5. Larson–Miller plot of MgO single crystal by constant strain rate compression.

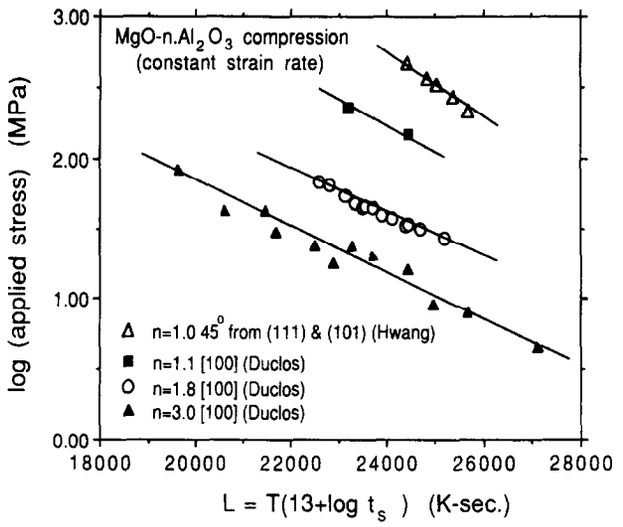

Fig. 6. Larson–Miller plot of spinel with different compositions.

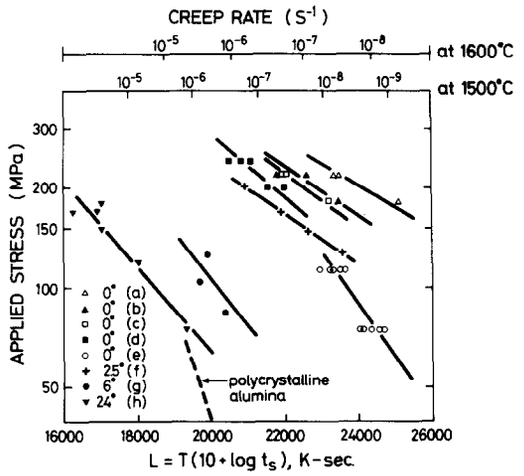

Fig. 7. Larson–Miller plot of sapphire fibres with different deviations from the c-axis. Upper scales indicate equivalent creep rates. Source references as follows: (a),(b),(c)[20], (d)[21], (e)[22], (f)[23] and (g)[24].

straight lines through the data. Where sufficient data is available, good correlation with the assumed linearity is observed. The constructed lines were then used to obtain the creep strength, i.e. the stress corresponding to $t_S = 10^4$s at a temperature of 1600°C. These conditions were based on a criterion for reinforcements in oxide–oxide composites proposed by Courtright.[2] As an example, for ThO_2 crystals (Fig. 3), the values of t_S and T give a Larson–Miller parameter of $L = 29968$ which gives by extrapolation creep strengths of 47 and 41 MPa for the [100] and [110] orientations respectively.

Creep data for crystals exhibiting the same C value can be displayed on plots with identical scales which permits direct comparison of the creep resistance of different crystals over the complete stress–temperature–life regime. This can be seen in Fig. 5 which demonstrates the sensitivity

Table 1. Creep strengths of some single crystal oxides (compression)

(a) Simple oxides

Oxides	*Direction of stress axis*	*Test temp. (°C)*	*Applied stress (MPa)*	*Test method*	*Test atmosp.*	C	*Creep strength (MPa)*	*Ref.*
BeO	$[1\bar{1}00]$	1650–1850	50–140	CLC	He	13	4	(3,4)
	$[11\bar{2}1]$	650–900	12–70	CLC	He	18	<1	(3,4)
MgO (Fe = 70 ppm)	<100>	1300–1500	20–70	CSC	Ar, CO/CO_2	14	2	(5)
MgO (Fe = 4300 ppm)	<100>	1300–1500	20–70	CSC	Ar, CO/CO_2	14	1	(5)
MgO (Fe = 11 900 ppm)	<100>	1300–1500	20–70	CSC	Ar, CO/CO_2	14	1	(5)
MgO	<100>	1665–1735	1·5–6	CSC	—	14	0·3	(6)
MgO	<100>	1300–1800	5–80	CSRC	He	14	3	(7)
	<111>	1700	37–96	CSRC	He	14	11	(7)
Al_2O_3	[0001]	1650–1850	140–400	CLC	He	11	64	(3)
	42° to [0001]	1200–1700	25–100	CLC	He	22	4	(3)
CaO	<111>	1200	5–50	CLC	—	10	1·2	(8)
	<100>	1200	8–40	CLC	—	10	0·6	(8)
CaO	<100>	1350–1450	5–15	CSC	Air	10	1·1	(9)
Y_2O_3	<110>	1550–1800	20–140	CLC	Air	10	36	(10)
YSZ*	[100]	1650–1850	12–100	CLC	Ar-2%H_2	14	16	(3)
	[110]	1650–1850	12–100	CLC	Ar-2%H_2	12	15	(3)
	$[1\bar{1}1]$	1650–1850	12–100	CLC	Ar-2%H_2	10	9	(3)
YSZ*	$[11\bar{2}]$	1300–1550	50–160	CLC	Air	21	13	(11)
YSZ*	<112>	1450–1750	59–300	CSRC	Air	21	44	(12)
					Ar	21	43	
ThO_2	[100]	1650–1850	50–100	CLC	Ar-2%H_2	12	47	(3)
	[110]	1650–1850	50–100	CLC	Ar-2%H_2	12	41	(3)
UO_2 (O/U=2·00	<100>	1100–1300	50–130	CSC	H_2	16	10	(13)
UO_2 (O/U=2·0001)	<100>	1100	80–130	CSC	H_2	16	24	(13)
UO_2 (O/U=2·001)	<100>	1100–1400	60–110	CSC	H_2	16	32	(13)
UO_2 (O/U=2·01)	<100>	1100–1300	50–90	CSC	H_2	16	22	(13)
UO_2 (O/U=2·121)	<100>	1100	30–70	CSC	H_2	16	12	13

(b) Complex oxides

Oxides	*Direction of stress axis*	*Test temp. (°C)*	*Applied stress (MPa)*	*Test method*	*Test atmosp.*	C	*Creep strength (MPa)*	*Ref.*
$BeAl_2O_4$	45° to [100]	1520–1620	25–100	CLC	Ar	18	2	(14)
	[100]	1520–1820	100–280	CLC	Ar	—	>280**	(14)
$MgO–0·9Al_2O_3$	[111]	1650–1850	50–200	CLC	He	11	33	(15)
	[100]	1650–1850	50–200	CLC	He	13	25	(15)
$MgO–Al_2O_3$	45° from (111) & (101)	1790–1850	200–480	CSRC	Ar	13	5	(16)
$MgO–1·1Al_2O_3$	[100]	1530–1630	150–230	CSRC	Ar	13	2·5	(17)
$MgO–1·8Al_2O_3$	[100]	1350–1650	20–70	CSRC	Ar	13	2·5	(17)
$MgO–3·0Al_2O_3$	[100]	1550–1850	5–90	CSRC	Ar	13	1	(17)
Mullite ($3Al_2O_3.2SiO_2$)	3° off c-axis	1400	480	CSC	Air	—	***	(18)
$Y_3Al_5O_{12}$ (YAG)	[110]	1650–1850	100–280	CLC	He	20	128	(3)
	[111]	1650–1850	100–280	CLC	He	20	135	(3)
	[100]	1650–1850	100–280	CLC	He	20	82	(3)

* Yttria stabilised zirconia.
** No detectable creep after 10 h at 1820°C and 280 MPa.
*** No detectable plastic strain at 1400° and 480 MPa for 200 h.
CLC = constant load compression; CSC = constant stress compression;
CSRC = constant strain rate compression (flow stresses were used in Larson–Miller plot for this test method).

of the creep of MgO to crystal orientation. Similarly, Fig. 6 reveals the sensitivity of the creep resistance of spinel to composition.

Figure 7 summarises tensile creep results for sapphire fibres; these have attracted considerable interest as potential reinforcement fibres. The figure illustrates the observed sharp decrease in creep resistance with angular deviation from *c*–axis loading but also a variation in the results from different sources. Such variation could in part be due to small variations in the axial orientation of fibres having a nominal *c*-axis orientation, reflecting the difficulty of growing the fibres with a precise orientation.

The effects revealed by the figures are also reflected in the creep strength values in Tables 1 and 2. Here it can also be seen that certain oxides such as Al_2O_3 and the binary oxides, $BeAl_2O_4$, yttrium aluminium garnet (YAG), mullite and spinel have very high creep resistance in certain crystal directions but exhibit extreme anisotropy. Others such as thoria and stabilised zirconia exhibit moderate strength with less anisotropy. Although there is small scope for direct comparison, the tensile creep results are fairly consistent with the compressive creep results, the former showing a tendency towards somewhat higher strengths. In general the results indicate that certain oxides show promise as high temperature reinforcements.

The creep mechanisms of the oxides are far from well understood and it is not the intention of this work to discuss possible explanations of the observed creep behaviour. Nevertheless, it is of interest to view the results in the light of the methodology proposed by Hillig[29] for predicting the mechanical properties of oxides at high temperature on the basis of such factors as the field strength of the cationic species, the apparent atomic volume of oxygen (V_O), the melting temperature and the crystal structure. Oxides having low values of V_O, high melting point and the most irregular and complicated crystal structure are predicted to offer the greatest strength, stiffness, creep resistance, and high temperature stability. On this basis certain oxides with complex structure, large shear moduli and large Burger's vector such as sapphire, YAG, spinel, mullite, chrysoberyl and BeO were considered to be the most promising candidates. In Table 3, several oxides are listed in the order of their melting points together with the upper and lower bound compressive creep strengths and details of their crystal structure. This confirms that the oxides with complicated structures, such as hexagonal, complex

Table 2. Creep strengths of single crystal oxides (tension)

Oxides	*Direction of stress axis*	*Test temp. (°C)*	*Applied stress (MPa)*	*Test method*	*Test atmosp.*	C	*Creep strength (MPa)*	*Ref.*
MgO	<011>	1200–1500	29–86·2	CLT	Air	10	5	(19)
Al_2O_3 (*c*–axis)	0°–[0001]	1700–1900	182–219	CST	Air	10	161	(20)
	0°–[0001]	1700–1900	182–219	CST	Air	10	138	(20)
Saphikon*	0°–[0001]	1700–1900	182–219	CST	Air	10	114	(20)
Mg–Ti doped	0°–[0001]	1700–1900	182–219	CST	Air	10	77	(20)
Cr–Ti doped	0°–[0001]	1700–1900	182–219	CST	Air	10	81	(20)
Al_2O_3 (*c*-axis)	0°–[0001]	1650–1800	200–240	CST	Air	10	120	(21)
	0°–[0001]	1600–1800	75–114	CST	Air	10	45	(22)
	2·5°–[0001]	1600–1800	132–204	CST	Air	10	89	(23)
	6°–[0001]	1600–1800	85–128	CST	Air	10	10	(23)
Saphikon*	24°–[0001]	1500	120–180	CST	Air	10	11	(24)
Al_2O_3 (*c*–axis)	<2°–[0001]	1760–1875	280–380	CSRT	Air	10	156	(25)
Ti^{4+} doped	<2°–[0001]	1800–1850	190–310	CSRT	Air	10	81	(26)
Sapphire (*a*–axis)	$<11\bar{2}0>$	1550–1850	90–245	CSRT	Vacuum	10	45	(27)
$MgAl_2O_4$ (spinel)	[110]	1871–1927	182–218	CLT	Air	10	70	(28)
YAG	[111]	1500–1850	200	CLT	Air	10	141**	(21)
	[100]	1500–1850	200	CLT	Air	10	~82**	(21)

* Saphikon is the trade name of a commercially-available sapphire fibre.
** Only one stress level. The Larson–Miller plot was drawn parallel to that of the YAG compression plot for the purpose of extrapolation.
CLT = constant load tension; CST = constant stress tension;
CSRT = constant strain rate tension (flow stresses were used in Larson–Miller plot for this test method).

Table 3. Relationship of creep strength with crystal structure and melting point

Oxides	*Crystal system & structure*	*Melting point (°C)*	*Highest creep strength (MPa)*	*Lowest creep strength (MPa)*
Mullite	Orthorhombic	1850	480 (1400°C, 200 h, no plastic deformation)	
$BeAl_2O_4$	Orthorhombic (Olivine)	1870	>280	2
YAG	Cubic (Complex bcc)	1950	135	94
Sapphire (Al_2O_3)	Hexagonal (hcp)	2001–2050	63	4
Spinel $MgO–0·9Al_2O_3$)	Cubic (Complex cubic)	2135	33	25
Y_2O_3	Cubic (Fluorite)	2401–2450 (Fluorite)	36	
BeO	Hexagonal (hcp)	2551–2600	41	<1
CaO	Cubic (NaCl)	2601–2650	1·2	0·6
YSZ	Cubic (α)	2715	14	9
MgO	Cubic (NaCl)	2751–2800	11	0·2
UO_2	Cubic (Fluorite)	2801–2850	32	10
ThO_2	Cubic (Fluorite)	3050	46	39

cubic and orthorhombic, exhibit superior creep resistance but as already noted are often very anisotropic. However, there is no obvious relationship between creep resistance and melting point. Thus, it seems that the effect of crystal structure overrides any correlation with melting point.

The extreme anisotropy of certain oxides presumably originates in an anisotropy of crystal and atomic bond structure. In this respect, a parallel can be drawn with carbon fibres in which the strong graphite basal atomic planes are oriented parallel to the fibre axis, leading to an extreme anisotropy of strength and stiffness in the fibres. In spite of their anisotropy, carbon fibres provide very successful reinforcement in composites, including carbon–carbon composites for high temperature applications.

4 Reliability of the Larson–Miller Procedure

The Larson–Miller method is a procedure that normalises creep data with respect to stress, temperature and strain rate. Its advantage over other normalisation approaches is that it permits convenient comparisons on the basis of relatively little data, only requiring the determination of two constants (the constant C and the slope of the log σ versus L plot). It may be suspected that this convenience is achieved at the expense of precision since the many variables involved in the creep processes are not accounted for individually. A more detailed description of the creep process used by Corman[3] is given by the semi-empirical power law equation:

$$\dot{\epsilon}_s = \frac{A_o D G b}{kT} (\sigma/G)^n \tag{6}$$

where A_o and n are constants, D is the appropriate diffusion coefficient, G the shear modulus, b the Burger's vector, k Boltzmann's constant, and σ is the applied stress. Putting

$$D = D_o \exp(-Q_D/RT) \tag{7}$$

where D_o is the frequency factor and Q_D the activation energy for the diffusion process, and:

$$G = G_o - (\Delta G)T \tag{8}$$

where G_o is the value of the shear modulus obtained by linear extrapolation to absolute zero, eqn (6) becomes after some rearrangement:

$$\dot{\epsilon}_s = A' \frac{G_o - (\Delta G)T}{kT} \left[\frac{\sigma}{G_o - (\Delta G)T}\right]^n \exp(-Q/RT) \tag{9}$$

where A' is a constant. For some of the oxides in Table 1, sufficient data was available for Corman to determine the values of A', Q_D and n by a regression analysis.[3] These values are listed in Table

Table 4. Comparison of the calculated results from semi-empirical equation with the results from Larson–Miller procedure

Oxides	*Direction*	A' *(K/MPa.S)*	n	Q_D *(J/mol)* $\times 10^3$	G_o *(MPa)* $\times 10^5$	ΔG *(MPa/K)*	*Stress (calculated with eqn 9) (MPa)*	*Stress (Larson–Miller method) (MPa)*
Sapphire	[0001]	$1{\cdot}9 \times 10^{7}$	4·54	470	1·70	24·3	63	64
Sapphire	42° to [000$\bar{1}$]	$1{\cdot}14 \times 10^{31}$	4·73	736	1·70	24·3	4	4
BeO	[1$\bar{1}$00]	$1{\cdot}33 \times 10^{15}$	3·38	496	1·654	18·5	39	41
BeO	[11$\bar{2}$1]	$2{\cdot}11 \times 10^{28}$	4·66	376	1·654	18·5	< 1	< 1
ThO_2	[100]	$5{\cdot}21 \times 10^{35}$	10·25	473	1·047	13·9	46	47
ThO_2	[110]	$3{\cdot}04 \times 10^{27}$	6·55	591	1·047	13·9	39	41
YSZ	[100]	$1{\cdot}25 \times 10^{17}$	3·86	519	0·645	18·6	14	16
YSZ	[110]	$3{\cdot}88 \times 10^{17}$	4·40	468	0·645	18·6	13	15
YSZ	[111]	$5{\cdot}56 \times 10^{14}$	3·85	406	0·645	18·6	9	9
YAG	[111]	$5{\cdot}94 \times 10^{25}$	5·64	710	1·195	7·2	115	135

*Values of A', n, Q_D, G_o and ΔG are from Corman.[3]

4 together with the associated values of creep strength calculated from eqn 9 with $\dot{\epsilon}_s = 10^{-9}$ s^{-1} and $T = 1873$ K, the latter being compared with the corresponding values derived using the Larson–Miller treatment. The agreement is sufficient to demonstrate that the Larson–Miller method offers a similar level of reliability.

5 Conclusions

The Larson–Miller method provides a convenient and effective means of comparing and ranking the creep resistance of oxides on the basis of results obtained under different stress and temperature conditions.

The creep of single crystals of several single and binary oxides was compared and it was found that binary oxides with complex crystal structures exhibited the highest creep strengths. However, these oxides were very anisotropic and the high strengths were found only for specific crystal orientations.

No clear correlation between the creep resistance of the oxides and their melting point could be seen.

References

1. Larson, F. R. & Miller, J., A time–temperature relationship for rupture and creep stresses. *Trans. ASME*, **74** (1952) 765–71.
2. Courtright, E. I., Engineering property limitations of structural ceramics and ceramic composites above 1600°C. *Ceram. Eng. Sci. Proc.*, **12**[9–10] (1991) 1725–44.
3. Corman, G. S., High-temperature creep of some single crystal oxides. *Ceram. Eng. Sci. Proc.*, **12**[9–10] (1991) 1745–66.
4. Corman, G. S., Creep of beryllia single crystals. *J. Am. Ceram. Soc.*, **75** (1992) 71–6.
5. Wolfenstine, J. & Kohlstedt, D. L., Creep of (Mg, Fe)O single crystals. *J. Mater. Sci.*, **23** (1988) 3550–7.
6. Ramesh, K. S., Yasuda, E. & Kimura, S., Negative creep and recovery during high-temperature creep of MgO single crystals at low stresses. *J. Mater. Sci.*, **21** (1986) 3147–52.
7. Routbort, J. L., Work hardening and creep of MgO. *Acta Metall.*, **27** (1979) 649–61.
8. Dixon-Stubbs, P. J. & Wilshire, B., Deformation processes during creep of single and polycrystalline CaO. *Phil. Mag. A*, **45** (1982) 519–29.
9. Duong, H. & Wolfenstine, J., Low-stress creep of single-crystalline calcium oxide. *J. Am. Ceram. Soc.*, **74** (1991) 2697–9.
10. Gaboriaud, P. R. J., High-temperature creep of yttrium sesquioxide: Y_2O_3. *Phil. Mag. A*, **44** (1981) 561–87.
11. Martinez-Fernandez, J., Jimenez-Melendo, M., Dominguez-Rodriguez, A. & Heuer, A. H., High-temperature creep of yttria-stabilised zirconia single crystals. *J. Am. Ceram. Soc.*, **73** (1990) 2452–6.
12. Jimenez-Melendo, M., Martinez-Fernandez, J., Dominguez-Rodriguez, A. & Castaing, J., Dislocation climb controlled deformation of Y_2O_3-doped cubic ZrO_2 single crystals. *J. Europ. Ceram. Soc.*, **12** (1993) 97–101.
13. Selterzer, M. S., Clauer, A. H. & Wilcox, B. A., The influence of stoichiometry on compression creep of uranium dioxide single crystals. *J. Nucl. Mater.*, **44** (1972) 43–56.
14. Whalen, P. J., Narasimhan, D., Gasdaska, C. G., O'Dell, E. W. & Morris, R. C., New high-temperature oxide composite reinforcement materials: chrysoberyl. *Ceram. Eng. Sci. Proc.*, **12**[9–10] (1991) 1774–84.
15. Corman, G. S., Creep of MgO-rich spinel single crystals. *J. Mater. Sci. Letters*, **11** (1992) 1657–60.
16. Hwang, L., Heuer, A. H. & Mitchell, T. E., Slip systems in stoichiometric $MgAl_2O_4$ spinel. In *Deformation of Ceramic Materials*, ed. R. C. Bradt & R. E. Tressler. Plenum, New York, 1975, pp. 257–70.
17. Duclos, R., Doukhan, N. & Escaig, B., Study of the origin of the composition influence on the mechanical properties of MgO Al_2O_3 spinels. *Acta Metall.*, **30** (1982) 1381–8.
18. Dokko, P. C., Pask, J. A. & Mazdiyasni, K. S., High-temperature mechanical properties of mullite under compression. *J. Am. Ceram. Soc.*, **60** (1977)150–5.
19. Clauer, A. H. & Wilcox, B. A., High temperature tensile creep of magnesium oxide single crystals. *J. Am. Ceram. Soc.*, **59** (1976) 89–96.
20. Haggerty, J. S., Wills, K. C. & Sheehan, J. E., Growth and poperties of single crystal oxide fibres. *Ceram. Eng. Sci. Proc.*, **12**[9–10] (1991) 1785–801.
21. Corman, G. S., Strength and creep of single crystal YAG fibres, Internal test report, General Electric Corporate Research and Development, Schenectady, NY, 1992.

22. Firestone, R. F., & Heuer, A. H., Creep deformation of 0° sapphire. *J. Am. Ceram. Soc.*, **59** (1976) 24–9.
23. Gooch, D. J., & Groves, G. W., The creep of sapphire filament with orientations close to the c–axis. *J. Mater. Sci.*, **8** (1973) 1238–46.
24. Porter, J. R., Reinforcements for ceramic–matrix composites for elevated temperatures. *Mater. Sci. Eng.*, **A166** (1993) 179–84.
25. Tressler, R. E. & Barber, D. J., Yielding and flow of c–axis sapphire filaments. *J. Am. Ceram. Soc.*, **57** (1974) 13–19.
26. Michael, D. J. & Tressler, R. E., Deformation dynamics of pore-free Ti^{4+}-doped and pure c–axis sapphire crystals. *J. Mater. Sci.*, **9** (1974) 1781–8.
27. Kotchick, D. M. & Tressler, R. E., Deformation behaviour of sapphire via the prismatic slip system. *J. Am. Ceram. Soc.*, **63** (1980) 429–34.
28. Sigalovsky, J., Wills, K. C., Haggerty, J. S. & Sheehan, J. E., Growth characteristics and properties of spinel single crystal fibres. *Ceram. Eng. Sci. Proc.*, **13**[7–8] (1992) 183–9.
29. Hillig, W. B., A methodology for estimating the mechanical properties of oxides at high temperatures. *J. Am. Ceram. Soc.*, **76** (1993) 129–38.